Progress In Electromagnetics Research, Vol. 130, 525–540, 2012

A NOVEL 3-D WEAKLY CONDITIONALLY STABLE FDTD ALGORITHM

J. Wang*, **B. Zhou, L. Shi, C. Gao, and B. Chen**

National Key Laboratory on Electromagnetic Environmental Effects and Electro-optical Engineering, PLA University of Science and Technology, Nanjing, China

Abstract—For analyzing the electromagnetic problems with the fine structures in one or two directions, a novel weakly conditionally stable finite-difference time-domain (WCS-FDTD) algorithm is proposed. By dividing the 3-D Maxwell's equations into two parts, and applying the Crank-Nicolson (CN) scheme to each part, a four sub-step implicit procedures can be obtained. Then by adjusting the operational order of four sub-steps, a novel 3-D WCS-FDTD algorithm is derived. The proposed method only needs to solve four implicit equations, and the Courant–Friedrich–Levy (CFL) stability condition of the proposed algorithm is more relaxed and only determined by one space discretisation. In addition, numerical dispersion analysis demonstrates the numerical phase velocity error of the weakly conditionally stable scheme is less than that of the 3-D ADI-FDTD scheme.

1. INTRODUCTION

The finite-difference time-domain (FDTD) method [1], which has been widely used for many years, is an effective and robust tool applicable to a wide variety of complex electromagnetic problems [2–11]. However, due to the upper limit on the time step size that needs to satisfy the Courant-Friedrich-Levy (CFL) stability condition, the computational efficiency of the conventional FDTD method is reduced, especially in analyzing the fine structures or the low frequency characteristics. To overcome this limit on the time step size, some unconditionally stable FDTD methods based on the Crank-Nicolson (CN) scheme [12–14] and the alternating-direction implicit (ADI) scheme [15–18] have been studied extensively. Although the time step sizes are no longer

Received 19 July 2012, Accepted 20 August 2012, Scheduled 23 August 2012
* Corresponding author: Jian-Bao Wang (yyuan5138@gmail.com).

bounded by the CFL stability condition, those unconditionally stable methods have less accuracy as the time step sizes are large and need to solve six implicit equations which become inefficient. In practice, some electromagnetic structures, such as patch antennas and shielding enclosure with thin slots, only have fine structures in one or two directions where fine grids are needed. For investigating the electromagnetic performances of those structures, some WCS-FDTD methods have been presented [19, 20].

In this paper, a novel WCS-FDTD algorithm which is suitable for problems with very fine structures in one or two directions is proposed. By splitting the 3-D Maxwell's equations into two parts, and applying the implicit scheme only in the two directions of fine structure where fine grids are needed in each part, a four sub-step implementations can be obtained. By adopting the proposed technology, the field advancement only needs to solve four implicit equations, and the time step size will no longer be bounded by the fine grid cell sizes, which is only determined by the large space discretisation. Numerical stability analysis demonstrates that the CFL stability condition of the proposed algorithm is more relaxed than those of the existing WCS-FDTD methods [19, 20], which means the proposed method is more efficient due to the larger time step size can be chose. Compared with the ADI-FDTD scheme, the numerical phase velocity error of the proposed algorithm is reduced, especially for large time-step size. Finally, numerical example is presented to illustrate its accuracy and efficiency.

2. IMPLEMENTATION OF THE PROPOSED METHOD

2.1. Formulation

Suppose that the time step size is only determined by the space step size along the x-direction. The 3-D Maxwell's equations can be split into two parts in matrix form as

$$\frac{\partial}{\partial t}\vec{\psi}_1 = [A_1]\,\vec{\psi}_1 + [B_1]\,\vec{\psi}_2 \tag{1a}$$

$$\frac{\partial}{\partial t}\vec{\psi}_2 = [A_2]\,\vec{\psi}_2 + [B_2]\,\vec{\psi}_1 \tag{1b}$$

where $\vec{\psi}_1 = [H_y, H_z, E_x]^{\mathrm{T}}$, $\vec{\psi}_2 = [E_y, E_z, H_x]^{\mathrm{T}}$,

$$[A_1] = \begin{pmatrix} 0 & 0 & -\frac{1}{\mu}\frac{\partial}{\partial z} \\ 0 & 0 & \frac{1}{\mu}\frac{\partial}{\partial y} \\ -\frac{1}{\varepsilon}\frac{\partial}{\partial z} & \frac{1}{\varepsilon}\frac{\partial}{\partial y} & 0 \end{pmatrix}, \quad [B_1] = \begin{pmatrix} 0 & \frac{1}{\mu}\frac{\partial}{\partial x} & 0 \\ -\frac{1}{\mu}\frac{\partial}{\partial x} & 0 & 0 \\ 0 & 0 & 0 \end{pmatrix},$$

$$[A_2] = \begin{pmatrix} 0 & 0 & \frac{1}{\varepsilon}\frac{\partial}{\partial z} \\ 0 & 0 & -\frac{1}{\varepsilon}\frac{\partial}{\partial y} \\ \frac{1}{\mu}\frac{\partial}{\partial z} & -\frac{1}{\mu}\frac{\partial}{\partial y} & 0 \end{pmatrix}, \quad [B_2] = \begin{pmatrix} 0 & -\frac{1}{\varepsilon}\frac{\partial}{\partial x} & 0 \\ \frac{1}{\varepsilon}\frac{\partial}{\partial x} & 0 & 0 \\ 0 & 0 & 0 \end{pmatrix}.$$

where ε and μ are the permittivity and permeability.

In (1a), by considering the set of field variables $\vec{\psi}_2$ as a correction term, and applying the CN scheme only to the set of field variables $\vec{\psi}_1$, we can get

$$\frac{\vec{\psi}_1^{n+1} - \vec{\psi}_1^{n}}{\Delta t} = [A_1] \frac{\vec{\psi}_1^{n+1} + \vec{\psi}_1^{n}}{2} + [B_1] \vec{\psi}_2^{n+\frac{1}{2}} \tag{2}$$

where Δt is the time step size. The above equation can be also written as

$$\left(I - \frac{\Delta t}{2}[A_1]\right) \vec{\psi}_1^{n+1} = \left(I + \frac{\Delta t}{2}[A_1]\right) \vec{\psi}_1^{n} + \Delta t\,[B_1]\,\vec{\psi}_2^{n+\frac{1}{2}}. \tag{3}$$

By splitting the space derivative operator $[A_1]$=$[C_1]$+$[D_1]$, (3) can be expressed as

$$\left(I-\frac{\Delta t}{2}[C_1]\right)\left(I-\frac{\Delta t}{2}[D_1]\right)\vec{\psi}_1^{n+1} = \left(I+\frac{\Delta t}{2}[C_1]\right)\left(I+\frac{\Delta t}{2}[D_1]\right)\vec{\psi}_1^{n}$$
$$+\Delta t\,[B_1]\,\vec{\psi}_2^{n+\frac{1}{2}} + \frac{\Delta t^2}{4}[C_1][D_1]\left(\vec{\psi}_1^{n+1} - \vec{\psi}_1^{n}\right). \tag{4}$$

After neglecting the Δt^2 term, we can get the approximation of the CN scheme known as the ADI scheme. (4) can be split into two sub-steps as

$$\left(I - \frac{\Delta t}{2}[C_1]\right)\vec{\psi}_1^{n+\frac{1}{2}} = \left(I + \frac{\Delta t}{2}[D_1]\right)\vec{\psi}_1^{n} + \frac{\Delta t}{2}[B_1]\,\vec{\psi}_2^{n+\frac{1}{2}} \tag{5}$$

$$\left(I - \frac{\Delta t}{2}[D_1]\right)\vec{\psi}_1^{n+1} = \left(I + \frac{\Delta t}{2}[C_1]\right)\vec{\psi}_1^{n+\frac{1}{2}} + \frac{\Delta t}{2}[B_1]\,\vec{\psi}_2^{n+\frac{1}{2}} \tag{6}$$

where

$$[C_1] = \begin{pmatrix} 0 & 0 & -\frac{1}{\mu}\frac{\partial}{\partial z} \\ 0 & 0 & 0 \\ -\frac{1}{\varepsilon}\frac{\partial}{\partial z} & 0 & 0 \end{pmatrix}, \quad [D_1] = \begin{pmatrix} 0 & 0 & 0 \\ 0 & 0 & \frac{1}{\mu}\frac{\partial}{\partial y} \\ 0 & \frac{1}{\varepsilon}\frac{\partial}{\partial y} & 0 \end{pmatrix}.$$

Similarly, the second part (1b) can be also split into a two sub-step procedures as

$$\left(I - \frac{\Delta t}{2}[C_2]\right)\vec{\psi}_2^{n+\frac{1}{2}} = \left(I + \frac{\Delta t}{2}[D_2]\right)\vec{\psi}_2^{n} + \frac{\Delta t}{2}[B_2]\,\vec{\psi}_1^{n+\frac{1}{2}} \tag{7}$$

$$\left(I - \frac{\Delta t}{2}[D_2]\right)\vec{\psi}_2^{n+1} = \left(I + \frac{\Delta t}{2}[C_2]\right)\vec{\psi}_2^{n+\frac{1}{2}} + \frac{\Delta t}{2}[B_2]\,\vec{\psi}_1^{n+\frac{1}{2}} \tag{8}$$

where

$$[C_2] = \begin{pmatrix} 0 & 0 & \frac{1}{\varepsilon}\frac{\partial}{\partial z} \\ 0 & 0 & 0 \\ \frac{1}{\mu}\frac{\partial}{\partial z} & 0 & 0 \end{pmatrix}, \quad [D_2] = \begin{pmatrix} 0 & 0 & 0 \\ 0 & 0 & -\frac{1}{\varepsilon}\frac{\partial}{\partial y} \\ 0 & -\frac{1}{\mu}\frac{\partial}{\partial y} & 0 \end{pmatrix}.$$

It is difficult to solve (5) and (7) as $\vec{\psi}_1$ and $\vec{\psi}_2$ are coupled together implicitly. To overcome this difficulty, we replace $\vec{\psi}_2^{n+\frac{1}{2}}$ in (5) and $\vec{\psi}_1^{n+\frac{1}{2}}$ in (8) by $\vec{\psi}_2^n$ and $\vec{\psi}_1^{n+1}$ respectively, and adjust the order of implementation as (5)→(7)→(6)→(8), then the four sub-step implementations can be got as

$$\left(I - \frac{\Delta t}{2}[C_1]\right)\vec{\psi}_1^{n+\frac{1}{2}} = \left(I + \frac{\Delta t}{2}[D_1]\right)\vec{\psi}_1^n + \frac{\Delta t}{2}[B_1]\vec{\psi}_2^n \tag{9a}$$

$$\left(I - \frac{\Delta t}{2}[C_2]\right)\vec{\psi}_2^{n+\frac{1}{2}} = \left(I + \frac{\Delta t}{2}[D_2]\right)\vec{\psi}_2^n + \frac{\Delta t}{2}[B_2]\vec{\psi}_1^{n+\frac{1}{2}} \tag{9b}$$

$$\left(I - \frac{\Delta t}{2}[D_1]\right)\vec{\psi}_1^{n+1} = \left(I + \frac{\Delta t}{2}[C_1]\right)\vec{\psi}_1^{n+\frac{1}{2}} + \frac{\Delta t}{2}[B_1]\vec{\psi}_2^{n+\frac{1}{2}} \tag{9c}$$

$$\left(I - \frac{\Delta t}{2}[D_2]\right)\vec{\psi}_2^{n+1} = \left(I + \frac{\Delta t}{2}[C_2]\right)\vec{\psi}_2^{n+\frac{1}{2}} + \frac{\Delta t}{2}[B_2]\vec{\psi}_1^{n+1}. \tag{9d}$$

The resulting equations of the above equations are written as First step:

$$H_y^{n+\frac{1}{2}}\left(i+\tfrac{1}{2}, j, k+\tfrac{1}{2}\right) - H_y^n\left(i+\tfrac{1}{2}, j, k+\tfrac{1}{2}\right) = a_1 \left[\frac{E_z^n\left(i+1,j,k+\frac{1}{2}\right) - E_z^n\left(i,j,k+\frac{1}{2}\right)}{\Delta x} - \frac{E_x^{n+\frac{1}{2}}\left(i+\frac{1}{2},j,k+1\right) - E_x^{n+\frac{1}{2}}\left(i+\frac{1}{2},j,k\right)}{\Delta z}\right] \tag{10a}$$

$$H_z^{n+\frac{1}{2}}\left(i+\tfrac{1}{2}, j+\tfrac{1}{2}, k\right) - H_z^n\left(i+\tfrac{1}{2}, j+\tfrac{1}{2}, k\right) = a_1 \left[\frac{E_x^n\left(i+\frac{1}{2},j+1,k\right) - E_x^n\left(i+\frac{1}{2},j,k\right)}{\Delta y} - \frac{E_y^n\left(i+1,j+\frac{1}{2},k\right) - E_y^n\left(i,j+\frac{1}{2},k\right)}{\Delta x}\right] \tag{10b}$$

$$E_x^{n+\frac{1}{2}}\left(i+\tfrac{1}{2}, j, k\right) - E_x^n\left(i+\tfrac{1}{2}, j, k\right) = a_2 \left[\frac{H_z^n\left(i+\frac{1}{2},j+\frac{1}{2},k\right) - H_z^n\left(i+\frac{1}{2},j-\frac{1}{2},k\right)}{\Delta y} - \frac{H_y^{n+\frac{1}{2}}\left(i+\frac{1}{2},j,k+\frac{1}{2}\right) - H_y^{n+\frac{1}{2}}\left(i+\frac{1}{2},j,k-\frac{1}{2}\right)}{\Delta z}\right]. \tag{10c}$$

Second step:

$$E_y^{n+\frac{1}{2}}\left(i, j+\tfrac{1}{2}, k\right) - E_y^n\left(i, j+\tfrac{1}{2}, k\right) = a_2 \left[\frac{H_x^{n+\frac{1}{2}}\left(i,j+\frac{1}{2},k+\frac{1}{2}\right) - H_x^{n+\frac{1}{2}}\left(i,j+\frac{1}{2},k-\frac{1}{2}\right)}{\Delta z} - \frac{H_z^{n+\frac{1}{2}}\left(i+\frac{1}{2},j+\frac{1}{2},k\right) - H_z^{n+\frac{1}{2}}\left(i-\frac{1}{2},j+\frac{1}{2},k\right)}{\Delta x}\right] \tag{11a}$$

$$E_z^{n+\frac{1}{2}}\left(i,j,k+\tfrac{1}{2}\right)-E_z^{n}\left(i,j,k+\tfrac{1}{2}\right)=a_2\left[\frac{H_y^{n+\frac{1}{2}}\left(i+\frac{1}{2},j,k+\frac{1}{2}\right)-H_y^{n+\frac{1}{2}}\left(i-\frac{1}{2},j,k+\frac{1}{2}\right)}{\Delta x}-\frac{H_x^{n}\left(i,j+\frac{1}{2},k+\frac{1}{2}\right)-H_x^{n}\left(i,j-\frac{1}{2},k+\frac{1}{2}\right)}{\Delta y}\right] \tag{11b}$$

$$H_x^{n+\frac{1}{2}}\left(i,j+\tfrac{1}{2},k+\tfrac{1}{2}\right)-H_x^{n}\left(i,j+\tfrac{1}{2},k+\tfrac{1}{2}\right)=a_1\left[\frac{E_y^{n+\frac{1}{2}}\left(i,j+\frac{1}{2},k+1\right)-E_y^{n+\frac{1}{2}}\left(i,j+\frac{1}{2},k\right)}{\Delta z}-\frac{E_z^{n}\left(i,j+1,k+\frac{1}{2}\right)-E_z^{n}\left(i,j,k+\frac{1}{2}\right)}{\Delta y}\right]. \tag{11c}$$

Third step:

$$H_y^{n+1}\left(i+\tfrac{1}{2},j,k+\tfrac{1}{2}\right)-H_y^{n+\frac{1}{2}}\left(i+\tfrac{1}{2},j,k+\tfrac{1}{2}\right)=a_1\left[\frac{E_z^{n+\frac{1}{2}}\left(i+1,j,k+\frac{1}{2}\right)-E_z^{n+\frac{1}{2}}\left(i,j,k+\frac{1}{2}\right)}{\Delta x}-\frac{E_x^{n+\frac{1}{2}}\left(i+\frac{1}{2},j,k+1\right)-E_x^{n+\frac{1}{2}}\left(i+\frac{1}{2},j,k\right)}{\Delta z}\right] \tag{12a}$$

$$H_z^{n+1}\left(i+\tfrac{1}{2},j+\tfrac{1}{2},k\right)-H_z^{n+\frac{1}{2}}\left(i+\tfrac{1}{2},j+\tfrac{1}{2},k\right)=a_1\left[\frac{E_x^{n+1}\left(i+\frac{1}{2},j+1,k\right)-E_x^{n+1}\left(i+\frac{1}{2},j,k\right)}{\Delta y}-\frac{E_y^{n+\frac{1}{2}}\left(i+1,j+\frac{1}{2},k\right)-E_y^{n+\frac{1}{2}}\left(i,j+\frac{1}{2},k\right)}{\Delta x}\right] \tag{12b}$$

$$E_x^{n+1}\left(i+\tfrac{1}{2},j,k\right)-E_x^{n+\frac{1}{2}}\left(i+\tfrac{1}{2},j,k\right)=a_2\left[\frac{H_z^{n+1}\left(i+\frac{1}{2},j+\frac{1}{2},k\right)-H_z^{n+1}\left(i+\frac{1}{2},j-\frac{1}{2},k\right)}{\Delta y}-\frac{H_y^{n+\frac{1}{2}}\left(i+\frac{1}{2},j,k+\frac{1}{2}\right)-H_y^{n+\frac{1}{2}}\left(i+\frac{1}{2},j,k-\frac{1}{2}\right)}{\Delta z}\right]. \tag{12c}$$

Fourth step:

$$E_y^{n+1}\left(i,j+\tfrac{1}{2},k\right)-E_y^{n+\frac{1}{2}}\left(i,j+\tfrac{1}{2},k\right)=a_2\left[\frac{H_x^{n+\frac{1}{2}}\left(i,j+\frac{1}{2},k+\frac{1}{2}\right)-H_x^{n+\frac{1}{2}}\left(i,j+\frac{1}{2},k-\frac{1}{2}\right)}{\Delta z}-\frac{H_z^{n+1}\left(i+\frac{1}{2},j+\frac{1}{2},k\right)-H_z^{n+1}\left(i-\frac{1}{2},j+\frac{1}{2},k\right)}{\Delta x}\right] \tag{13a}$$

$$E_z^{n+1}\left(i,j,k+\tfrac{1}{2}\right)-E_z^{n+\frac{1}{2}}\left(i,j,k+\tfrac{1}{2}\right)=a_2\left[\frac{H_y^{n+1}\left(i+\frac{1}{2},j,k+\frac{1}{2}\right)-H_y^{n+1}\left(i-\frac{1}{2},j,k+\frac{1}{2}\right)}{\Delta x}-\frac{H_x^{n+1}\left(i,j+\frac{1}{2},k+\frac{1}{2}\right)-H_x^{n+1}\left(i,j-\frac{1}{2},k+\frac{1}{2}\right)}{\Delta y}\right] \tag{13b}$$

$$H_x^{n+1}\left(i,j+\tfrac{1}{2},k+\tfrac{1}{2}\right)-H_x^{n+\frac{1}{2}}\left(i,j+\tfrac{1}{2},k+\tfrac{1}{2}\right)=a_1\left[\frac{E_y^{n+\frac{1}{2}}\left(i,j+\frac{1}{2},k+1\right)-E_y^{n+\frac{1}{2}}\left(i,j+\frac{1}{2},k\right)}{\Delta z}-\frac{E_z^{n+1}\left(i,j+1,k+\frac{1}{2}\right)-E_z^{n+1}\left(i,j,k+\frac{1}{2}\right)}{\Delta y}\right]. \tag{13c}$$

where $a_1 = \Delta t/2\mu$ and $a_2 = \Delta t/2\varepsilon$.

In the first step, only two field components $H_y^{n+\frac{1}{2}}$ and $E_x^{n+\frac{1}{2}}$ are coupled implicitly. To decouple them, by substituting (10a) into (10c) the implicit equation for $E_x^{n+\frac{1}{2}}$ is obtained as

$$\begin{aligned}
&\left(1+2\frac{a_1a_2}{\Delta z^2}\right)E_x^{n+\frac{1}{2}}\left(i+\frac{1}{2},j,k\right)\\
&-\frac{a_1a_2}{\Delta z^2}\left[E_x^{n+\frac{1}{2}}\left(i+\frac{1}{2},j,k+1\right)+E_x^{n+\frac{1}{2}}\left(i+\frac{1}{2},j,k-1\right)\right]\\
=\;&E_x^n\left(i+\frac{1}{2},j,k\right)+\frac{a_2}{\Delta y}\left[H_z^n\left(i+\frac{1}{2},j+\frac{1}{2},k\right)-H_z^n\left(i+\frac{1}{2},j-\frac{1}{2},k\right)\right]\\
&-\frac{a_2}{\Delta z}\left[H_y^n\left(i+\frac{1}{2},j,k+\frac{1}{2}\right)-H_y^n\left(i+\frac{1}{2},j,k-\frac{1}{2}\right)\right]-\frac{a_1a_2}{\Delta x\Delta z}\\
&\left[E_z^n\left(i+1,j,k+\frac{1}{2}\right)-E_z^n\left(i+1,j,k-\frac{1}{2}\right)\right.\\
&\left.-E_z^n\left(i,j,k+\frac{1}{2}\right)+E_z^n\left(i,j,k-\frac{1}{2}\right)\right] \qquad (14)
\end{aligned}$$

Updating $E_x^{n+\frac{1}{2}}$ using (14) only requires solving a tridiagonal matrix, which is quite efficient. Then $H_y^{n+\frac{1}{2}}$ and $H_z^{n+\frac{1}{2}}$ can be calculated explicitly by using (10a) and (10b) respectively.

When $H_y^{n+\frac{1}{2}}$ and $H_z^{n+\frac{1}{2}}$ are obtained, in the second step only $H_x^{n+\frac{1}{2}}$ and $E_y^{n+\frac{1}{2}}$ are coupled implicitly. By substituting (11a) into (11c) the implicit equation for $H_x^{n+\frac{1}{2}}$ is given as

$$\begin{aligned}
&\left(1+2\frac{a_1a_2}{\Delta z^2}\right)H_x^{n+\frac{1}{2}}\left(i,j+\frac{1}{2},k+\frac{1}{2}\right)\\
&-\frac{a_1a_2}{\Delta z^2}\left[H_x^{n+\frac{1}{2}}\left(i,j+\frac{1}{2},k+\frac{3}{2}\right)+H_x^{n+\frac{1}{2}}\left(i,j+\frac{1}{2},k-\frac{1}{2}\right)\right]\\
=\;&H_x^n\left(i,j+\frac{1}{2},k+\frac{1}{2}\right)+\frac{a_1}{\Delta z}\left[E_y^n\left(i,j+\frac{1}{2},k+1\right)-E_y^n\left(i,j+\frac{1}{2},k\right)\right]\\
&-\frac{a_1}{\Delta y}\left[E_z^n\left(i,j+1,k+\frac{1}{2}\right)-E_z^n\left(i,j,k+\frac{1}{2}\right)\right]-\frac{a_1a_2}{\Delta x\Delta z}\\
&\left[H_z^{n+\frac{1}{2}}\left(i+\frac{1}{2},j+\frac{1}{2},k+1\right)-H_z^{n+\frac{1}{2}}\left(i+\frac{1}{2},j+\frac{1}{2},k\right)\right.\\
&\left.-H_z^{n+\frac{1}{2}}\left(i-\frac{1}{2},j+\frac{1}{2},k+1\right)+H_z^{n+\frac{1}{2}}\left(i-\frac{1}{2},j+\frac{1}{2},k\right)\right]. \qquad (15)
\end{aligned}$$

$H_x^{n+\frac{1}{2}}$ can be obtained also by solving a tridiagonal matrix using (15). With the approximate solutions for $H_x^{n+\frac{1}{2}}$, $H_y^{n+\frac{1}{2}}$ and $H_z^{n+\frac{1}{2}}$, the magnetic field components $E_y^{n+\frac{1}{2}}$ and $E_z^{n+\frac{1}{2}}$ can be obtained explicitly by using (11a) and (11b) respectively.

Similarly, the field components of the $n+1$ time step can be computed using the simultaneous equations of the third and fourth step in the same way.

2.2. Numerical Stability Analysis

The stability can be analyzed by the Fourier method [21, 22]. Using the plane wave solution of the Maxwell's equations, the amplification factor ξ from n to $n+\frac{1}{2}$ and from $n+\frac{1}{2}$ to $n+1$ can be solved as

From n to $n+\frac{1}{2}$:

$$\xi_{1,2} = 1, \quad \xi_{3,4} = \frac{2 - m_1^2 \pm \sqrt{\left(2 - m_1^2\right)^2 - 4\left(1 + m_2^2\right)\left(1 + m_3^2\right)}}{2\left(1 + m_3^2\right)}.$$

From $n+\frac{1}{2}$ to $n+1$:

$$\xi_{5,6} = 1, \quad \xi_{7,8} = \frac{2 - m_1^2 \pm \sqrt{\left(2 - m_1^2\right)^2 - 4\left(1 + m_2^2\right)\left(1 + m_3^2\right)}}{2\left(1 + m_2^2\right)}.$$

where $m_1 = c\Delta t \sin(k_x \Delta x/2)/\Delta x$, $m_2 = c\Delta t \sin(k_y \Delta y/2)/\Delta y$, $m_3 = c\Delta t \sin(k_z \Delta z/2)/\Delta z$, k_x, k_y and k_z are wave numbers, and c is the speed of light in the medium.

While $(2 - m_1^2)^2 \leq 4$ as well as $\Delta t \leq 2\Delta x/c$, the magnitude of the amplification factor is

$$\begin{aligned} |\xi| &= |\xi_{3,4}| \times |\xi_{7,8}| \\ &= \left| \frac{2 - m_1^2 \pm i\sqrt{4(1 + m_2^2)(1 + m_3^2) - \left(2 - m_1^2\right)^2}}{2(1 + m_2^2)} \right| \\ &\quad \times \left| \frac{2 - m_1^2 \pm i\sqrt{4\left(1 + m_2^2\right)\left(1 + m_3^2\right) - \left(2 - m_1^2\right)^2}}{2\left(1 + m_3^2\right)} \right| = 1. \end{aligned}$$

It can be seen that the magnitude of the amplification factor $|\xi|$ is unity and, thus, the CFL stability condition of the proposed method is $\Delta t \leq 2\Delta x/c$, which is more relaxed than that of the existing WCS-FDTD method ($\Delta t \leq \Delta x/c$) [20]. As we know, the CFL stability condition of the conventional FDTD method is $\Delta t \leq 1\Big/\left(c\sqrt{1/\Delta x^2 + 1/\Delta y^2 + 1/\Delta z^2}\right)$ [22]. By contrast, we set $\Delta x = 10\Delta y = 10\Delta z$, the ratio $\Delta t_1/\Delta t_2 = 2\sqrt{201} \approx 28.4$, where Δt_1

and Δt_2 are the maximum allowed time step sizes of the proposed method and the conventional FDTD method respectively. As a result, the proposed method has a greater advantage in the computational efficiency, especially for the problems with very fine structures in one or two directions.

2.3. Numerical Dispersion Analysis

By using the method presented in [22], the numerical dispersion relations of the proposed method and the ADI-FDTD method are as follows.

Numerical dispersion relation of the proposed method:

$$\cos(\omega\Delta t) = \frac{2 + m_1^4 - 4m_1^2 - 2m_2^2 - 2m_3^2 - 2m_2^2 m_3^2 + m_1^2 m_2^2 m_3^2}{2\left(1 + m_2^2\right)\left(1 + m_3^2\right)}. \quad (16)$$

Numerical dispersion relation of the ADI-FDTD method:

$$\cos(\omega\Delta t) = \frac{1 - m_1^2 - m_2^2 - m_3^2 - m_1^2 m_2^2 - m_2^2 m_3^2 - m_1^2 m_3^2 + m_1^2 m_2^2 m_3^2}{\left(1 + m_1^2\right)\left(1 + m_2^2\right)\left(1 + m_3^2\right)}. \quad (17)$$

Suppose that a wave is propagating at angles θ and φ, which is shown in Figure 7. By substituting $k_x = \cos\theta$, $k_y = \sin\theta\cos\varphi$ and $k_z = \sin\theta\sin\varphi$ into the dispersion relations (16) and (17) respectively, the numerical phase velocity $v_p = w/k$ related with θ and φ can be obtained.

Firstly, the uniform cell ($\Delta x = \Delta y = \Delta z$) is considered, and the cell size is set to be $\lambda/20$, where λ is the wavelength of simulation.

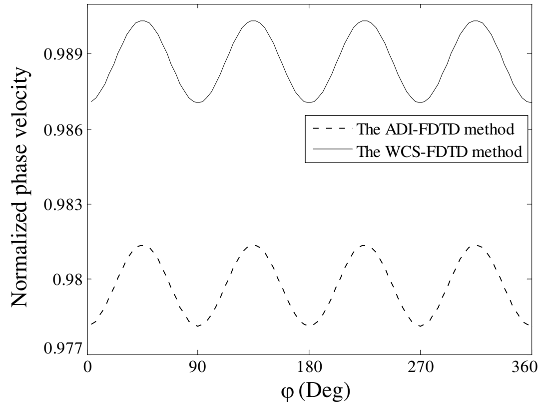

Figure 1. Normalized phase velocity varying with φ from 0° to 360° as θ=45°, $\Delta x = \Delta y = \Delta z = \lambda/20$ and $\Delta t = 2\Delta x/c$.

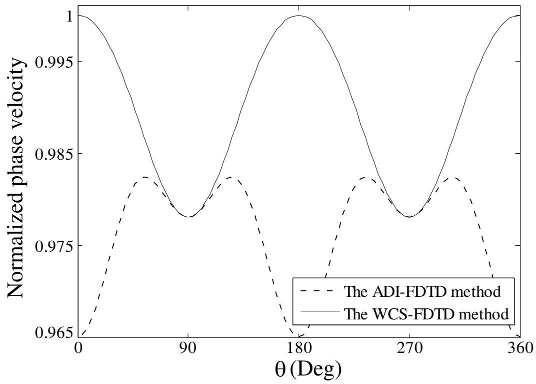

Figure 2. Normalized phase velocity varying with θ from 0° to 360° as φ=45°, $\Delta x = \Delta y = \Delta z = \lambda/20$ and $\Delta t = 2\Delta x/c$.

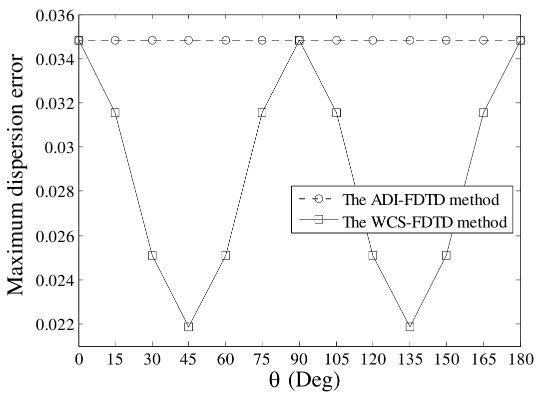

Figure 3. Maximum normalized dispersion error varying with θ from 0° to 180° as $\Delta x = \Delta y = \Delta z = \lambda/20$ and $\Delta t = 2\Delta x/c$.

As the time step size is set to be $\Delta t = 2\Delta x/c$, the normalized phase velocities varying with θ and φ are shown in Figures 1 and 2 respectively, and the maximum normalized dispersion error varying with θ is shown in Figure 3. When a nonuniform cell ($\Delta x = 10\Delta y = 10\Delta z = \lambda/15$) is adopted, the normalized phase velocities varying with θ and φ are shown in Figures 4 and 5 respectively, and the maximum normalized dispersion error varying with θ is shown in Figure 6.

From Figures 1–6 it can be seen that the dispersion error of the proposed method is less than that of the ADI-FDTD method, which demonstrates that the proposed method has a high accuracy.

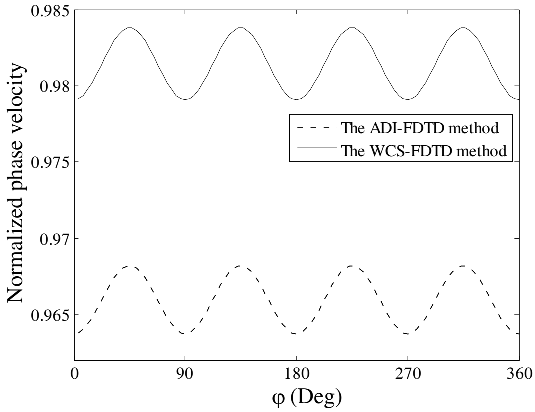

Figure 4. Normalized phase velocity varying with φ from 0° to 360° as θ=45°, $\Delta x = 10\Delta y = 10\Delta z = \lambda/15$ and $\Delta t = 2\Delta x/c$.

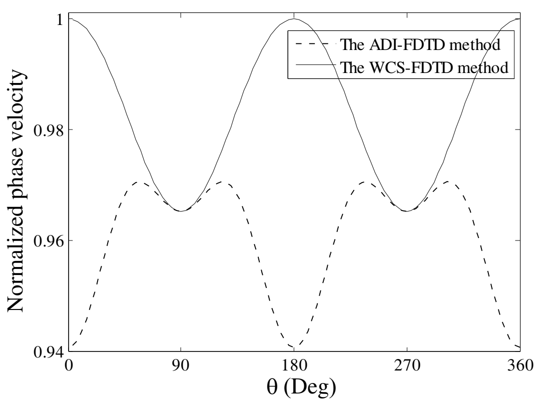

Figure 5. Normalized phase velocity varying with θ from 0° to 360° as φ=45°, $\Delta x = 10\Delta y = 10\Delta z = \lambda/15$ and $\Delta t = 2\Delta x/c$.

3. NUMERICAL VALIDATION

For the sake of simplicity and verifications, a rectangular cavity shown in Figure 7 was investigated with the conventional FDTD scheme, the ADI-FDTD scheme and the proposed FDTD scheme. The cavity has the dimension of 30 cm × 10 cm × 10 cm. A nonuniform mesh $\Delta x = 5\Delta y = 5\Delta z = 1$ cm was used, leading to a total number of $30 \times 50 \times 50$ cells.

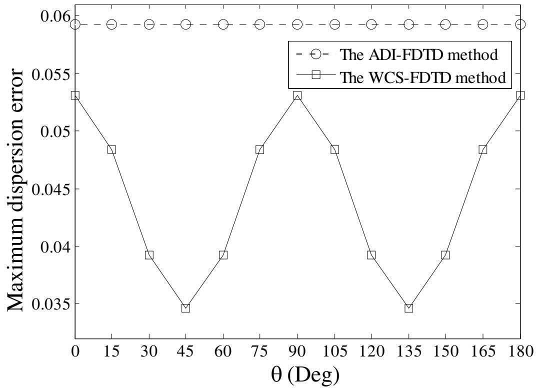

Figure 6. Maximum normalized dispersion error varying with θ from $0°$ to $180°$ as $\Delta x = 10\Delta y = 10\Delta z = \lambda/15$ and $\Delta t = 2\Delta x/c$.

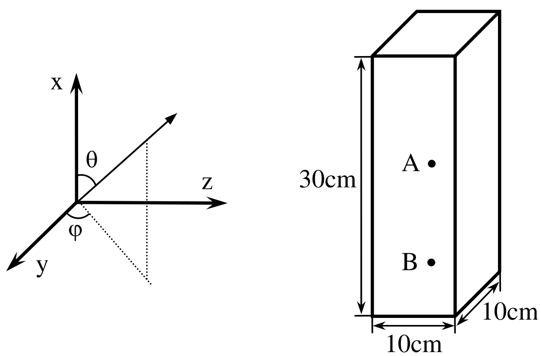

Figure 7. Geometry of a rectangular cavity.

3.1. Numerical Accuracy

A short current source applied along the z-direction is placed at the central point of the cavity. The Gaussian pulse function is adopted as the excitation, which is:

$$I_i\left(t\right) = \exp\left(-\frac{4\pi\left(t - t_0\right)^2}{\tau^2}\right)$$

where $\tau = 40\Delta x/c$ and $t_0 = 0.8\tau$. The observation point B is set 10 cm far from the source point A along the x-direction.

In the numerical example, the conventional FDTD method was used as a benchmark to verify the accuracy of the proposed method. Due to the limitation of the CFL stability condition, the time step size of the conventional FDTD was chosen as $\Delta t =$

$1\Big/\Big(c\sqrt{1/\Delta x^2+1/\Delta y^2+1/\Delta z^2}\Big) \approx \Delta x/7.2c$. For the comparison purpose, the time step sizes of the ADI-FDTD method and the WCS-FDTD method were chosen $\Delta t = \Delta x/2.4c$, $\Delta t = \Delta x/1.2c$ and $\Delta t = \Delta x/0.6c$. At the three cases, the waveforms of the electric field component E_z sampled at point B were shown in Figures 8, 9 and 10 respectively, and the maximum relative errors between the conventional FDTD method and the ADI-FDTD method (the WCS-FDTD method) were given in Table 1.

From Figures 8–10 and Table 1 it can be obviously observed that the proposed method has a higher accuracy than the ADI-FDTD method. At small time step size, the errors of two methods are relatively little. However, as increasing the size of time step, the error of the ADI-FDTD increases more rapidly than the proposed method. This is due to the less dispersion error of the proposed method.

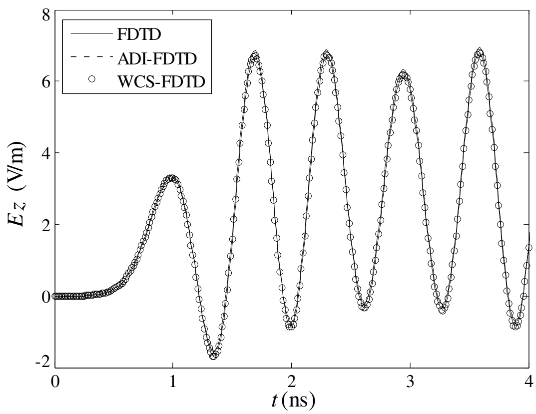

Figure 8. E_z calculated by the conventional FDTD method ($\Delta t = \Delta x/7.2c$), the ADI-FDTD method ($\Delta t = \Delta x/2.4c$) and the proposed method ($\Delta t = \Delta x/2.4c$).

Table 1. The maximum relative errors of the ADI-FDTD method and The WCS-FDTD method.

Time step sizes	**Maximum relative errors**	
	ADI-FDTD	WCS-FDTD
$\Delta t = \Delta x/2.4c$	3.017%	0.927%
$\Delta t = \Delta x/1.2c$	10.901%	2.289%
$\Delta t = \Delta x/0.6c$	49.595%	8.275%

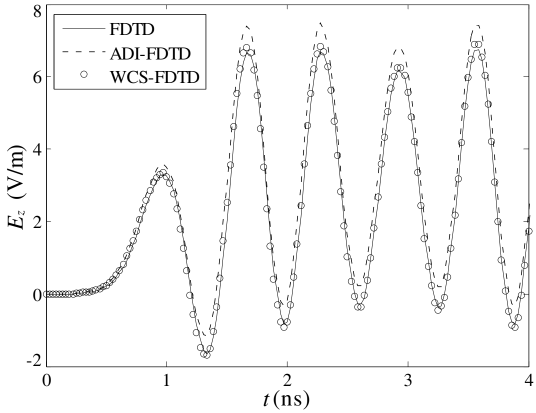

Figure 9. E_z calculated by the conventional FDTD method ($\Delta t = \Delta x/7.2c$), the ADI-FDTD method ($\Delta t = \Delta x/1.2c$) and the proposed method ($\Delta t = \Delta x/1.2c$).

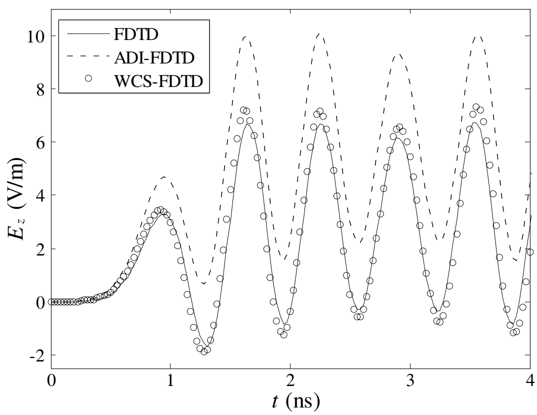

Figure 10. E_z calculated by the conventional FDTD method ($\Delta t = \Delta x/7.2c$), the ADI-FDTD method ($\Delta t = \Delta x/0.6c$) and the proposed method ($\Delta t = \Delta x/0.6c$).

3.2. Computational Efficiency

Because only four implicit equations are needed to be solve, the proposed WCS-FDTD method is more efficient than the ADI-FDTD method. In addition, due to more relaxed CFL stability condition, the CPU time of the proposed is more saving than the conventional FDTD method, especially for analyzing problems with very fine structures in one or two directions. Table 2 shows the CPU times of three methods

Table 2. The CPU times of numerical simulations using the conventional FDTD method, the ADI-FDTD method and the proposed WCS-FDTD method.

	$\Delta t = \Delta x/7.2c$	$\Delta t = \Delta x/2.4c$	$\Delta t = \Delta x/1.2c$	$\Delta t = \Delta x/0.6c$
FDTD	42.154			
ADI-FDTD	104.802	36.137	18.387	9.275
WCS-FDTD	76.142	26.255	13.358	6.737

at three cases, which demonstrates that the proposed method has a more computational efficiency.

4. CONCLUSION

In this paper, we present a novel weakly conditionally stable FDTD method which is very suitable for problems with very fine structures in one or two directions. The CFL stability condition of the proposed method is more relaxed and only determined by one space discretisation. By compared with the ADI-FDTD method, the numerical phase velocity error of the proposed scheme is much less. Numerical example demonstrates that the proposed WCS-FDTD method has a higher accuracy and efficiency.

ACKNOWLEDGMENT

This work was supported by the National Natural Science Foundation of China under Grants 60971063 and 51077133.

REFERENCES

1. Yee, K. S., "Numerical solution of initial boundary value problems involving Maxwell's equations in isotropic media," *IEEE Trans. Antennas Propag.*, Vol. 14, No. 3, 302–307, 1966.
2. Lei, J.-Z., C.-H. Liang, and Y. Zhang, "Study on shielding effectiveness of metallic cavities with apertures by combining parallel FDTD method with windowing technique," *Progress In Electromagnetics Research*, Vol. 74, 85–112, 2007.
3. Yang, S., Y. Chen, and Z.-P. Nie, "Simulation of time modulated linear antenna arrays using the FDTD method," *Progress In Electromagnetics Research*, Vol. 98, 175–190, 2009.

4. Hadi, M. F. and S. F. Mahmoud, "Optimizing the compact-FDTD algorithm for electrically large waveguiding structures," *Progress In Electromagnetics Research*, Vol. 75, 253–269, 2007.
5. Xiao, S.-Q., Z. Shao, and B.-Z. Wang, "Application of the improved matrix type FDTD method for active antenna analysis," *Progress In Electromagnetics Research*, Vol. 100, 245–263, 2010.
6. Li, J., L.-X. Guo, and H. Zeng, "FDTD method investigation on the polarimetric scattering from 2-D rough surface," *Progress In Electromagnetics Research,* Vol. 101, 173–188, 2010.
7. Vaccari, A., A. Cala' Lesina, L. Cristoforetti, and R. Pontalti, "Parallel implementation of a 3D subgridding FDTD algorithm for large simulations," *Progress In Electromagnetics Research*, Vol. 120, 263–292, 2011.
8. Izadi, M., M. Z. A. Ab Kadir, and C. Gomes, "Evaluation of electromagnetic fields associated with inclined lightning channel using second order FDTD-hybrid methods," *Progress In Electromagnetics Research,* Vol. 117, 209–236, 2011.
9. Sirenko, K., V. Pazynin, Y. K. Sirenko, and H. Bağci, "An FFT-accelerated FDTD scheme with exact absorbing conditions for characterizing axially symmetric resonant structures," *Progress In Electromagnetics Research*, Vol. 111, 331–364, 2011.
10. Lee, K. H., I. Ahmed, R. S. M. Goh, E. H. Khoo, E. P. Li, and T. G. G. Hung, "Implementation of the FDTD method based on lorentz-Drude dispersive model on gpu for plasmonics applications," *Progress In Electromagnetics Research*, Vol. 116, 441–456, 2011.
11. Kong, Y.-D. and Q.-X. Chu, "Reduction of numerical dispersion of the six-stages split-step unconditionally-stable FDTD method with controlling parameters," *Progress In Electromagnetics Research*, Vol. 122, 175–196, 2012.
12. Sun, G. and C. W. Trueman, "Efficient implementations of the Crank-Nicolson scheme for the finite-difference time-domain method," *IEEE Trans. Microwave Theory Tech.*, Vol. 54, No. 5, 2275–2284, 2006.
13. Xu, K., Z. Fan, D.-Z. Ding, and R.-S. Chen, "GPU accelerated unconditionally stable Crank-Nicolson FDTD method for the analysis of three-dimensional microwave circuits," *Progress In Electromagnetics Research*, Vol. 102, 381–395, 2010.
14. Rouf, H. K., F. Costen, S. G. Garcia, and S. Fujino, "On the solution of 3-D frequency dependent crank-nicolson FDTD scheme," *Journal of Electromagnetic Waves and Applications*, Vol. 23, No. 16, 2163–2175, 2009.

15. Zheng, F., Z. Chen, and J. Zhang, "Toward the development of a three-dimensional unconditionally stable finite-difference time-domain method," *IEEE Trans. Microw. Theory Tech.*, Vol. 48, No. 9, 1550–1558, 2000.
16. Namiki, T., "3-D ADI-FDTD method-unconditionally stable time-domain algorithm for solving full vector Maxwell's equations," *IEEE Trans. Microwave Theory Tech.*, Vol. 48, No. 10, 1743–1748, 2000.
17. Tay, W. C. and E. L. Tan, "Implementations of PMC and PEC boundary conditions for efficient fundamental ADI and LOD-FDTD," *Journal of Electromagnetic Waves and Application*, Vol. 24, No. 4, 565–573, 2010.
18. Shi, Y., L. Li, and C.-H. Liang, "The ADI multi-domain pseudospectral time-domain algorithm for 2-D arbitrary inhomogeneous media," *Journal of Electromagnetic Waves and Applications*, Vol. 19, No. 4, 543–558, 2005.
19. Huang, B. K., G. Wang, Y. S. Jiang, and W. B. Wang, "A hybrid implicit-explicit FDTD scheme with weakly conditional stability," *Microw. Opt. Tech. Lett.*, Vol. 39, 97–101, 2003.
20. Chen, J. and J. G. Wang, "A novel WCS-FDTD method with weakly conditional stability," *IEEE Trans. Electomag. Compat.*, Vol. 49, No. 2, 419–429, 2007.
21. Thomas, J. W., *Numerical Partial Differential Equations: Finite Difference Methods*, Springer Verlag, Berlin, Germany, 1995.
22. Taflove, A. and S. C. Hagness, *Computational Electrodynamics: The Finite-Difference Time-Domain Method*, 2nd Edition, Artech House, Norwood, MA, 2000.